OPEN

Activation of Cannabinoid Receptors Attenuates Endothelin-1–Induced Mitochondrial Dysfunction in Rat Ventricular Myocytes

Yan Lu, PhD,† Danielle I. Lee, PhD,*† Subir Roy Chowdhury, MD, PhD,‡ Ping Lu, PhD,§ Amit Kamboj, PhD,‡ Christopher M. Anderson, PhD,§¶ Paul Fernyhough, PhD,‡¶ and Hope D. Anderson, PhD*†¶*

Abstract: Evidence suggests that the activation of the endocannabinoid system offers cardioprotection. Aberrant energy production by impaired mitochondria purportedly contributes to various aspects of cardiovascular disease. We investigated whether cannabinoid (CB) receptor activation would attenuate mitochondrial dysfunction induced by endothelin-1 (ET1). Acute exposure to ET1 (4 hours) in the presence of palmitate as primary energy substrate induced mitochondrial membrane depolarization and decreased mitochondrial bioenergetics and expression of genes related to fatty acid oxidation (ie, peroxisome proliferator–activated receptor-gamma coactivator-1α, a driver of mitochondrial biogenesis, and carnitine palmitoyltransferase-1β, facilitator of fatty acid uptake). A CB1/CB2 dual agonist with limited brain penetration, CB-13, corrected these parameters. AMP-activated protein kinase (AMPK), an important regulator of energy homeostasis, mediated the ability of CB-13 to rescue mitochondrial function. In fact, the ability of CB-13 to rescue fatty acid oxidation–related bioenergetics, as well as expression of proliferator-activated receptor-gamma coactivator-1α and carnitine palmitoyltransferase-1β, was abolished by pharmacological inhibition of AMPK using compound C and shRNA knockdown of AMPKα1/α2, respectively. Interventions that target CB/AMPK signaling might represent a novel therapeutic approach to address the multifactorial problem of cardiovascular disease.

Key Words: cardiac myocyte, endothelin-1, endocannabinoid, mitochondria

(*J Cardiovasc Pharmacol*™ 2020;75:54–63)

INTRODUCTION

Endocannabinoids are endogenous polyunsaturated fatty acids that bind to cannabinoid receptors to elicit physiological effects. These G-protein–coupled receptors include CB1 and CB2 receptor subtypes. Both CB1 and CB2 receptors are present in the cardiovascular system (ie, heart[1,2] and blood vessels[3,4]), although CB1 and CB2 receptors are also profusely expressed in the brain[5] and immune cells.[6]

Aside from CB receptors, other constituents of the endocannabinoid signaling system are present in the heart. These include endocannabinoid ligands, such as arachidonoylethanolamide (AEA or anandamide)[7] and 2-arachidonoylglycerol (2-AG),[8] and the enzyme fatty acid amide hydrolase,[9,10] which hydrolyzes anandamide and 2-AG.[10,11]

Manipulating the endocannabinoid system may be a salutary approach worth pursuing, as endocannabinoid signaling plays a diverse role in modulating central and peripheral physiology.[12] In fact, extant evidence suggests that cannabinoids are protective in the ischemic heart. For example, infarct size is reduced by endogenous and synthetic cannabinoid agonists,[13,14] reportedly via CB2,[15] and this was associated with recovery of ventricular function.[13,14] We also previously reported that cannabinoid receptor signaling prevents cardiac myocyte hypertrophy.[16] Here, we extended these findings by determining the effects of CB receptor activation on mitochondrial function.

The heart requires a large amount of adenosine triphosphate (ATP), for which mitochondria are the major source. In the healthy heart, cardiac myocytes use predominantly fatty acids as energy substrate, and this accounts for 50%–70% of total ATP production.[17,18] The electron transport chain (ETC) embedded within the mitochondrial inner membrane is responsible for oxidative phosphorylation, thereby yielding approximately 95% of the total ATP.[19] Accordingly, mitochondria

Received for publication February 27, 2019; accepted September 4, 2019.

From the *College of Pharmacy, Rady Faculty of Health Sciences, University of Manitoba, Winnipeg, Manitoba, Canada; †Canadian Centre for Agri-Food Research in Health and Medicine, St. Boniface Hospital Research Centre, Winnipeg, Manitoba, Canada; ‡Division of Neurodegenerative Disorders, St. Boniface Hospital Research Centre, Winnipeg, Manitoba, Canada; §Neuroscience Research Program, Kleysen Institute for Advanced Medicine, Winnipeg Health Sciences Centre and Max Rady College of Medicine, University of Manitoba, Winnipeg, Manitoba, Canada; and ¶Department of Pharmacology and Therapeutics, Max Rady College of Medicine, University of Manitoba, Winnipeg, Manitoba, Canada.

Supported by the Canadian Institutes of Health Research (MOP 130297) and studentships from the Manitoba Health Research Council/St. Boniface Hospital Foundation (Y.L.) and Canadian Institutes of Health Research (D.I.L.).

The authors report no conflicts of interest.

Supplemental digital content is available for this article. Direct URL citations appear in the printed text and are provided in the HTML and PDF versions of this article on the journal's Web site (www.jcvp.org).

Y. Lu and D. I. Lee co-first author.

Reprints: Hope D. Anderson, PhD, College of Pharmacy, Rady Faculty of Health Sciences, University of Manitoba, 750 McDermot Avenue, Winnipeg, Manitoba, Canada R3E 0T5 (e-mail: handerson@sbrc.ca).

constitute a significant 30% of cardiac myocyte volume.[20] Given this key role, mitochondrial dysfunction has been linked to ischemia reperfusion injury,[21] cardiomyopathy,[22] left ventricular hypertrophy,[23] and heart failure.[24]

Here, we determined the early effects of endothelin-1 (ET1) on mitochondrial membrane permeability, membrane polarization, and bioenergetics in cardiac myocytes, in the presence of fatty acids as primary energy substrate. Furthermore, we tested the hypothesis that CB receptor signaling would rescue mitochondrial function and probed the signaling pathway(s) involved.

MATERIALS AND METHODS

Materials

Endothelin-1 (ET1), compound C, β-actin antibody, L-carnitine hydrochloride, oligomycin, carbonylcyanide 4-(trifluoromethoxy) phenylhydrazone (FCCP), rotenone, antimycin A, and etomoxir were from Sigma Aldrich (St Louis, MO). CB-13 and the JC-1 mitochondrial membrane potential assay kit were from Cayman Chemical (Ann Arbor, MI). Calcein-AM (Molecular Probes) and carnitine palmitoyltransferase (CPT)-1β primers were from Life Technologies (Carlsbad, CA). p-AMPKα (Thr172) and AMPKα antibodies were from Cell Signaling (2535S and 2603S, respectively; Whitby, Canada). CB1 and CB2 antibodies were from Abcam (ab23703 and ab45942, respectively; Toronto, Canada). Proliferator-activated receptor-gamma coactivator (PGC)-1α antibody was from EMD Millipore (ST1202; Temecula, CA). XF24 FluxPaks were from Agilent (Santa Clara, CA).

Neonatal Rat Ventricular Myocytes

This study was approved by the University of Manitoba Animal Care Committee and follows Canadian Council of Animal Care guidelines. Ventricular myocytes were isolated from 1-day-old neonatal Sprague Dawley rats by digestion with several cycles of 0.1% trypsin and mechanical disruption, as previously described.[25] Cells were cultured on gelatin-coated plates in Dulbecco's Modified Eagle Medium containing 10% cosmic calf serum (Hyclone) for 18–24 hours before experimentation.

Treatments

As applicable, myocytes were subjected to lentiviral infection. Myocytes were rendered quiescent by serum deprivation for 24 hours and then exposed to ET1 (0.1 μM; 4 hours) in the presence or absence of vehicle, CB-13 (1 μM), and/or a chemical inhibitor of AMPK (compound C; 1 μM; 1 hour). The concentration of ET1 (0.1 μM) is predicated on our extensive use of neonatal rat cardiac myocytes treated with ET1 as our experimental paradigm of cardiac myocyte hypertrophy.[26–28] Accordingly, we used this experimental paradigm to generate our finding that ligand activation of cannabinoid receptors attenuates hypertrophy of neonatal rat cardiomyocytes.[16] Here, this concentration of ET1 increased hypertrophic parameters (myocyte cell size and fetal gene activity) in an AMPK-dependent manner.[16] The 4-hour incubation time is based first, on the literature precedent in which Sun et al[29] reported disruption of mitochondrial function in pulmonary arterial endothelial cells after 4 hours, and second, time course experiments, in which we found that CB-13 significantly activated AMPK at 4 hours.[16] Ligands remained in the culture media for the remainder of the experiment. CB-13 is a nonselective CB1/CB2 agonist with limited brain penetration (Ki: CB1 = 6.1 nM vs. CB2 = 27.9 nM).[30,31] The concentration of CB-13 was selected based on, first, our finding that it attenuates myocyte hypertrophy,[16] and second, that micromolar plasma concentrations are achievable following oral administration of CB-13 (3 mg/kg).[30] Levels of CB1 and CB2 receptor expression are unaffected by CB-13 in the presence or absence of ET1 (see **Figure S6**, **Supplemental Digital Content 1**, http://links.lww.com/JCVP/A425).

shRNA Knockdown of AMPKα

Lentiviral vectors expressing shRNA against AMPK α_1 and α_2 were prepared, as previously described.[16] Myocytes were infected for 24 hours, and then cultured for a further 72 hours to allow knockdown before further experimentation. Degree of knockdown was confirmed by Western blotting (see **Figure S5**, **Supplemental Digital Content 1**, http://links.lww.com/JCVP/A425).

Measurement of Mitochondrial Respiration

An XF24 Analyzer (Agilent) was used to measure mitochondrial bioenergetics. The XF24 creates a reversible 7-μL enclosure above cells; this facilitates real-time monitoring of oxygen consumption rate (OCR) before reequilibration with the unenclosed incubation medium.[32,33] Fatty acid–dependent OCRs, driven by palmitate/bovine serum albumin (BSA) conjugate, were measured under basal conditions. Briefly, myocytes were seeded at 100,000 cells per well and exposed to assay media 1 hour before the assay. Independent experiments were conducted using distinct neonatal myocyte preparations to generate an n-value ≥3 (5 replicates per n-value). Krebs–Henseleit buffer containing L-carnitine hydrochloride (0.4 mM), glucose (2.5 mM), and palmitate/BSA conjugate (200 μM) was used to measure fatty acid–dependent respiration. Following the measurement of basal OCR, oligomycin (1 μg/mL), FCCP (palmitate assays —10 μM), and rotenone + antimycin A (1 μM each) were sequentially injected. Oligomycin is an ATP synthase inhibitor and eliminates OCR associated with ATP synthesis (ATP-linked OCR). Remaining OCR represents oxygen consumption attributable to proton leak. Mitochondrial coupling efficiency is the ratio of ATP-linked OCR to basal OCR. FCCP is a protonophore that uncouples the ETC and allows protons to flow back into the mitochondrial matrix to reduce oxygen. Thus, OCR in the presence of FCCP reflects maximal respiratory capacity, and the difference between maximal OCR and basal OCR reflects spare respiratory capacity. Finally, rotenone + antimycin A abolishes electron flow through complexes I–III, preventing oxygen consumption by cytochrome c oxidase. The remaining OCR in this case is the result of nonmitochondrial respiration.[33] Nonmitochondrial respiration was subtracted during the calculation of all bioenergetic parameters, as previously described.[32,33] The CPT1 inhibitor, etomoxir (40 μM), was used to verify that

fatty acid–dependent respiration was the result of oxidation of exogenous palmitate, and BSA served as negative control. OCR is represented as picomoles per minute per 10-μg protein and is expressed as % untreated control. The aforementioned experimental conditions are predicated on optimization experiments (see **Figures S1–S4**, **Supplemental Digital Content 1**, http://links.lww.com/JCVP/A425), showing that OCR peaked at a seeding density of 75,000–100,000 cells per well, as previously reported,[34] that reduction in OCR by oligomycin is concentration dependent, and that the maximal effect of FCCP on fatty acid oxidation (FAO) was achieved at 10 μM. Also, etomoxir (40 μM) dramatically inhibited palmitate-related OCR, and BSA only generated negligible OCR, thereby confirming that oxygen consumption was the result of oxidation of exogenous palmitate.

Measurement of Mitochondrial Membrane Permeability Transition

Calcein-AM and $CoCl_2$ dual staining is a well-established method used to assess the extent of membrane permeability transition (mPT) in intact cells.[35] Calcein-AM is a membrane-permeant dye that, upon entry into the cell, is converted to green fluorescent calcein by intracellular esterases. $CoCl_2$ selectively quenches cytosolic calcein fluorescence, thereby improving detection of bright fluorescent calcein puncta within mitochondria. Mitotracker-Red (0.1 μM) was also coloaded, and overlap between calcein and Mitotracker-Red verified mitochondrial localization of calcein puncta (images not shown). When mPT pores (pPTPs) open, calcein leaks from mitochondria into the cytosol, thereby decreasing the fluorescence contrast between mitochondria and cytosol.

Myocytes were cultured in 48-well plates (0.25×10^6 cells/well) and pretreated with CB-13 (1 μM; 1 hour) or vehicle in Krebs–Henseleit buffer supplemented with palmitate/BSA substrates (200 μM), L-carnitine hydrochloride (0.4 mM), and glucose (2.5 mM). Myocytes were then coloaded with calcein-AM (2 μM), $CoCl_2$ (2 mM), and MitoTracker-Red (0.1 μM) for 15 minutes, followed by a 5-minute wash with phosphate-buffered saline. The excitation/emission wavelengths for calcein and MitoTracker-Red are 494/517 nm and 579/599 nm, respectively. Images were acquired using an Olympus inverted fluorescence microscope before and after treatment (ie, 0 and 15 minutes) with ET1 (0.1 μM) or vehicle. Fluorescence contrast was determined as the difference in fluorescent calcein intensity between mitochondria (eg, puncta) and cytosol using Image J. For each replicate, images were captured for 5 myocytes, and within each myocyte, fluorescent calcein intensity was quantified in 3 separate fields within mitochondria. Results are presented as percent values of posttreatment:pretreatment fluorescence contrast. Cells were incubated with ionomycin (2 μM) for 5 minutes at the end of the experiment; this causes mPT and served as positive control.

Mitochondrial Membrane Potential ($\Delta\psi_m$) Imaging

The lipophilic fluorescent probe JC-1 was used to investigate changes in $\Delta\psi_m$, as per the manufacturer's protocol. In healthy mitochondria with relatively high $\Delta\psi_m$, JC-1 concentrates as J-aggregates and emits red fluorescence. In contrast, in mitochondria with reduced $\Delta\psi_m$, JC-1 presents mainly as monomeric form because of decreased concentration and emits green fluorescence. The ratio of aggregate to monomer fluorescence serves as an indicator of changes in $\Delta\psi_m$.

Myocytes were loaded with JC-1 for 60 minutes at 37°C in Krebs–Henseleit buffer containing palmitate/BSA substrates (200 μM), L-carnitine hydrochloride (0.4 mM), and glucose (2.5 mM) to assess fatty acid–dependent $\Delta\psi_m$. Myocytes were then washed with phosphate-buffered saline for 5 minutes, and images were acquired using an Olympus inverted fluorescence microscope. Samples were excited at 485 nm for monomer fluorescence and at 560 nm for JC-1 aggregate fluorescence. Emission fluorescence images were recorded at 535 nm for JC-1 monomer and 595 nm for JC-1 aggregates. Fluorescence intensity was also quantified using a SpectraMax Gemini XS fluorescence microplate reader. Also, as JC-1 may respond to plasma membrane depolarization, FCCP (1 μM) was added at the end of each experiment to achieve maximal dissipation of $\Delta\psi_m$ and served as positive control.

Western Blotting

Myocytes were cultured in 6-well plates (2×10^6 cells/well). Following treatments, cell lysates were prepared in radioimmune precipitation assay buffer and clarified by centrifugation. Antibodies against p-AMPK (1:1000), AMPK (1:1000), and PGC-1α (1:1000) were used for the detection by conventional Western blotting. Membranes were stripped and reprobed with β-actin antibody to account for loading variations among lanes.

RNA Extraction and Real-Time Polymerase Chain Reaction

Myocytes were cultured in 12-well plates (1×10^6 cells/well). Following treatments, total RNA was extracted from myocytes using the RNeasy mini kit (QIAGEN, Hilden, Germany). Real-time polymerase chain reaction (PCR) was performed using the iScript One-Step RT-PCR SYBR Green kit (Bio-Rad, ON, Canada) in the presence of CPT-1β primers (forward: 5′-CTTCTCAGTATGGTTCATCTTCTC-3′; reverse: 5′-CGAACATCCACCCATGATAG-3′). Glyceraldehyde 3-phosphate dehydrogenase was employed as the internal control (forward: 5′-CTCATGACCACAGTCCATGC-3′; reverse: 5′-TTCAGCTCTGGGATGACCT-3′).

Statistics

Data are presented as mean ± SEM. As applicable, 1-way analysis of variance, followed by a Newman–Keuls or Dunn Multiple Comparison test, was used to detect between-group differences. P value of < 0.05 was considered significant.

RESULTS

CB-13 attenuates ET1-induced aberrations of FAO-related mitochondrial bioenergetics. As shown in Figure 1,

ET1 reduced a number of bioenergetic parameters pertaining to FAO using palmitate, including (vs. control) basal OCR (82% ± 5%; $P < 0.05$), coupling efficiency (86% ± 6%; $P < 0.05$), maximal (78% ± 4%; $P < 0.01$) and spare (72% ± 5%; $P < 0.01$) respiratory capacity, and respiratory control ratio (81% ± 5%; $P < 0.01$). Basal OCR consists of both ATP-linked and proton leak–linked OCR; Figures 1C, D suggest that reduction in basal OCR was solely attributable to a decrease in ATP-linked OCR (74% ± 7%; $P < 0.05$ vs. control). CB-13 pretreatment partially attenuated the depression of basal OCR (95% ± 3%, not significant (ns) vs. control nor ET1) and coupling efficiency (97% ± 2%, ns vs. control nor ET1), and significantly restored maximal (97% ± 5%, $P < 0.05$ vs. ET1) and spare respiratory capacity (97% ± 4%, $P < 0.01$ vs. ET1), as well as respiratory control ratio (94% ± 2%, $P < 0.05$ vs. ET1). Proton leak–related OCR was unaffected by either ET1 or CB-13.

AMPK contributes to CB-13–dependent correction of FAO-related mitochondrial bioenergetics in hypertrophied myocytes. AMPK maintains or promotes ATP production by improving FAO.[36,37] Thus, we queried whether AMPK mediates preservation of FAO by CB-13. CB-13 effects on FAO-dependent bioenergetics in ET1-treated myocytes were abolished by a chemical inhibitor of AMPK, compound C.

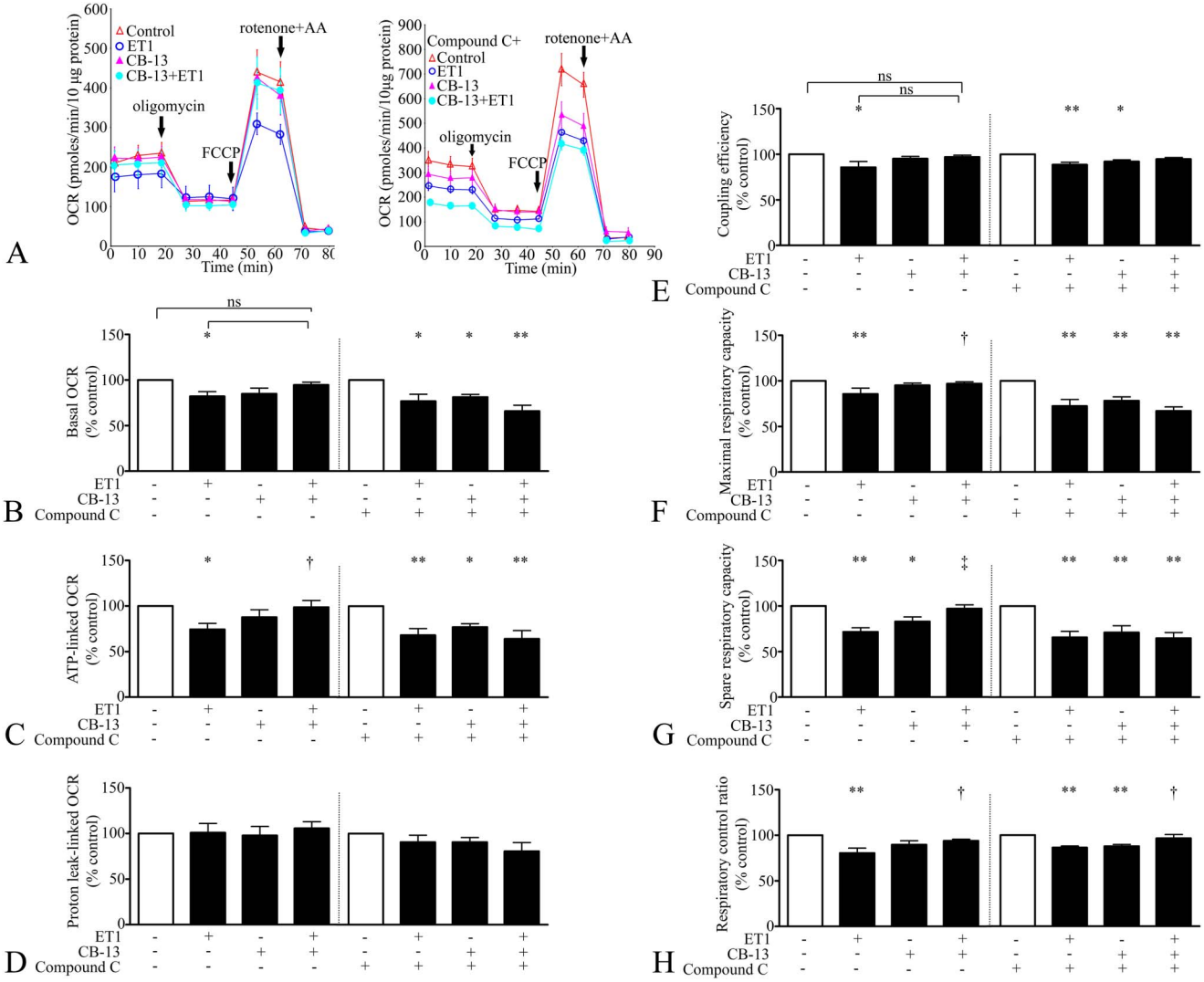

FIGURE 1. CB-13 attenuates ET1-induced depression of FAO-related respiration. Serum-deprived myocytes were pretreated with CB-13 (1 μM; 2 hours) followed by the addition of ET1 (0.1 μM; 4 hours) and provided palmitate/BSA conjugates (200 μM) as energy substrate. A, Representative plots. Left panel B–G, quantitative data demonstrate that ET1 reduced (B) basal OCR, (C) ATP-linked OCR, (E) coupling efficiency, (F) maximal, and (G) spare respiratory capacity, as well as (H) respiratory control ratio. CB-13 attenuated ET1 effects. D, Proton leak–linked OCR was unaffected by ET1 or CB-13. Right panel B–G, quantitative data demonstrate that the ability of CB-13 to attenuate ET1-induced reductions in (B) basal OCR, (C) ATP-linked OCR, (E) coupling efficiency, (F) maximal, and (G) spare respiratory capacity were attenuated, at least in part, by compound C. D, Proton leak–linked OCR and (H) respiratory control ratio were unaffected. n = 4–7 (5 replicates/n); *$P < 0.05$ and **$P < 0.01$ versus control (open bars); ns = not significant; †$P < 0.05$ and ‡$P < 0.01$ versus ET1. Mean ± SEM.

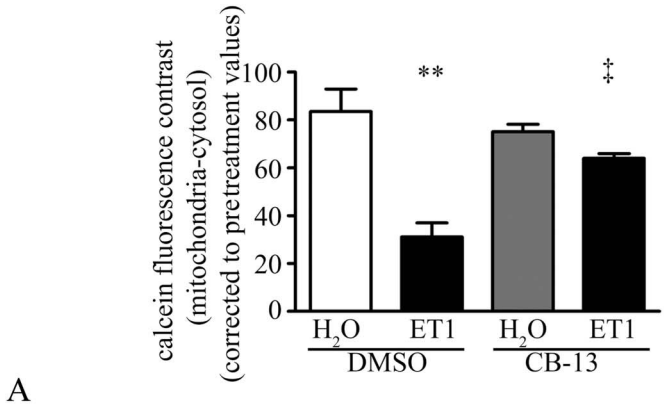

A

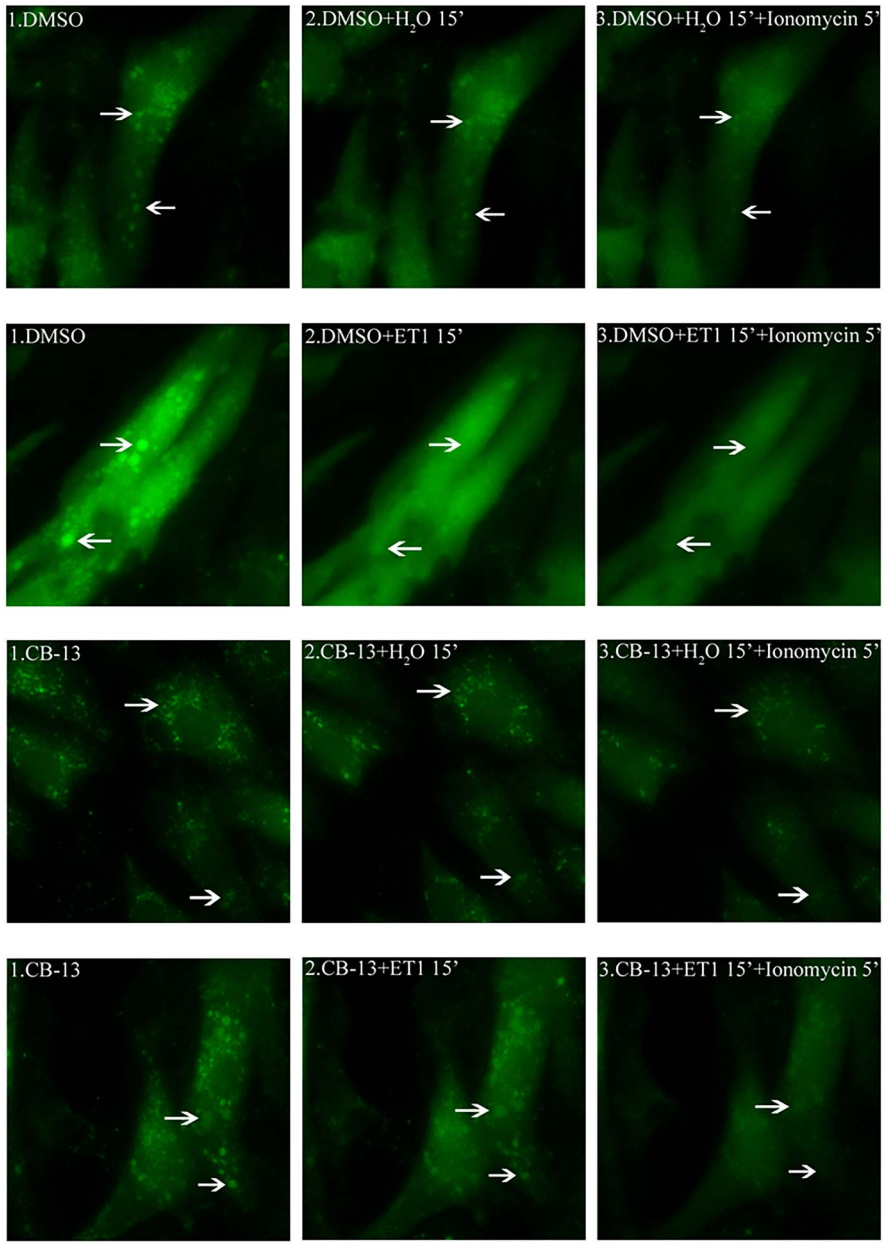

B

FIGURE 2. CB-13 ameliorates ET1-induced mPT. Serum-deprived myocytes were pretreated with CB-13 (1 μM, 1 hour) or DMSO (vehicle for CB-13), followed by the addition of ET1 (0.1 μM, 15 minutes) or H_2O in media containing palmitate/BSA (200 μM) as substrate. Calcein fluorescence contrast between mitochondria and cytosol, an indicator that negatively correlates with mPT, was measured within randomly selected myocytes before (t = 0 minutes) and after (t = 15 minutes) ET1/H_2O treatments. A, Results are presented as percent of post-treatment:pretreatment fluorescent contrast. Addition of ET1 (0.1 μM) to myocytes for 15 minutes significantly dissipated fluorescence calcein contrast between mitochondria and cytosol compared with H_2O-treatment, suggesting increased mPT. In the presence of CB-13 (1 μM), ET1 failed to reduce fluorescence calcein contrast between mitochondria and cytosol, suggesting preserved mPT. B, Representative fluorescent images, arrows indicate regions of calcein fluorescence contrast between mitochondria and cytosol. n = 3.15 mitochondrial regions from 5 myocytes were analyzed per replicate. $^{**}P < 0.01$ versus H_2O treatment with DMSO (open bar); ‡$P < 0.01$ versus ET1 treatment with DMSO. Mean ± SEM. DMSO, dimethyl sulfoxide.

We first determined that compound C treatment alone (1 μM) did not affect bioenergetic parameters (data not shown). However, in the presence of compound C, CB-13 failed to rescue (vs. control) basal OCR (66% ± 6%; $P < 0.01$), ATP-linked OCR (64% ± 9%; $P < 0.01$), and maximal (67% ± 4%; $P < 0.01$) and spare (65% ± 6%; $P < 0.01$) respiratory capacity (Fig. 1) in ET1-treated myocytes. Interestingly, fatty acid–related respiration was also impaired in the CB-13 + compound C group (vs. control), as shown by reduced basal OCR (81% ± 3%; $P < 0.05$), ATP-linked OCR (77% ± 4%; $P < 0.05$), coupling efficiency (92% ± 2%; $P < 0.05$), maximal (78% ± 4%; $P < 0.01$) and spare (71% ± 7%; $P < 0.01$) respiratory capacity, and respiratory control ratio (88% ± 2%; $P < 0.01$) (Fig. 1).

ET1-Induced mPT is Prevented by CB-13

Myocytes were first pretreated with CB-13 or its vehicle, dimethyl sulfoxide, followed by loading of calcein-AM and $CoCl_2$. Images were acquired before (t = 0 minutes) and after treatment (t = 15 minutes) with ET1 or H_2O. Fluorescence contrast between mitochondria and cytosol was measured to reflect the status of mPTPs. Lower fluorescence contrast indicates greater calcein leak from mitochondria to cytosol, and it is evidence of higher levels of mPT. As shown in Figure 2, ET1 induced a significant reduction in fluorescence contrast compared with H_2O (ET1: 31% ± 6% vs. H_2O: 84% ± 9%; $P < 0.01$), suggesting an increase in mPT. In contrast, myocytes pretreated with CB-13 exhibited similar fluorescence contrast after treatment with H_2O or ET1 (ET1: 64% ± 2% vs. H_2O: 75% ± 3%, not significant), suggesting that CB-13 prevented ET1-dependent mPT. At the end of the experiment, myocytes from all groups were treated with ionomycin (2 μM; 5 minutes). Ionomycin causes Ca^{2+} overload and induces mPT and thus served as positive control. Mitochondrial fluorescence puncta were dissipated by ionomycin in all groups (data not shown).

CB-13 Prevents ET1-Induced Mitochondrial Membrane Depolarization in an AMPK-Independent Manner

The ratio of red J-aggregates to green monomer declined in ET1-treated cells (80% ± 3%; $P < 0.05$ vs. control), reflecting membrane depolarization (Fig. 3A). Depolarization was attenuated by CB-13 pretreatment (106% ± 10%; $P < 0.05$ vs. ET1). The ability of CB-13 to prevent mitochondrial depolarization was unaffected by the AMPK chemical inhibitor, compound C (Fig. 3B).

CB-13 Attenuates ET1-Reduced Expression of PGC-1α and CPT-1β Through AMPK

CB-13 treatment (4 hours) increased phosphorylation of AMPKα at Thr172 (303% ± 60%; $P < 0.01$ vs. control) (Fig. 4A), which is an indicator of AMPK activation status.[38,39] PGC-1α, a central regulator of mitochondrial metabolism,[40] was reduced by ET1 by 41% ± 7% ($P < 0.01$ vs. control), and this was prevented by CB-13 (96% ± 2%; $P < 0.05$ vs. ET1). CB-13 alone increased PGC-1α (140% ± 27%;

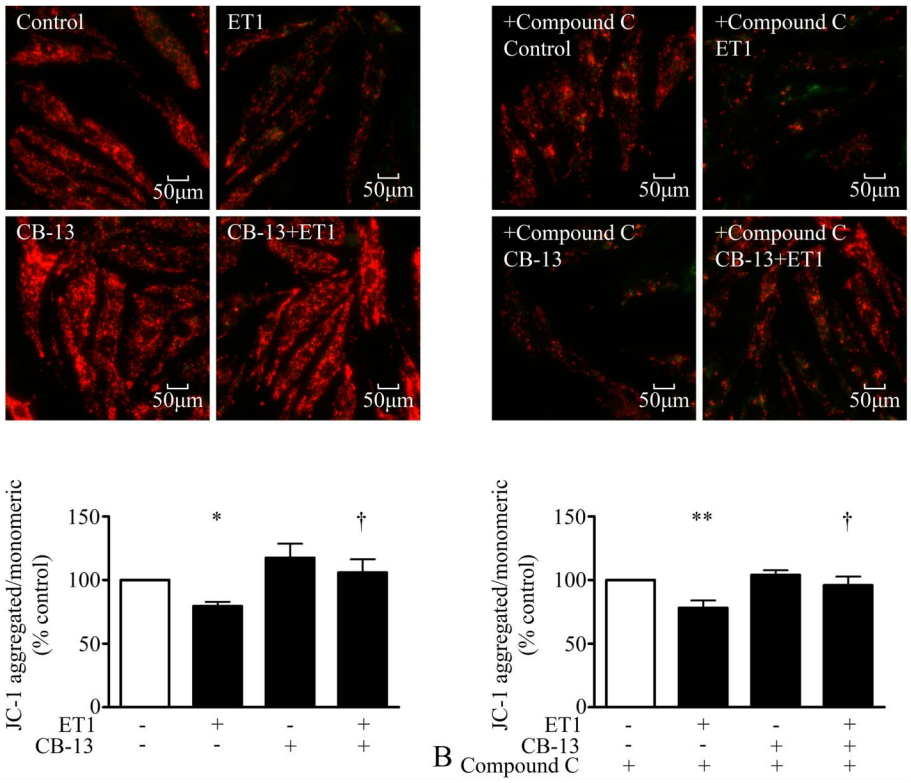

FIGURE 3. In the presence of palmitate as energy substrate, CB-13 prevents ET1-induced mitochondrial membrane depolarization in an AMPK-independent manner. Serum-deprived myocytes were pretreated with CB-13 (1 μM, 2 hours) in the presence or absence of compound C (AMPK inhibitor, 1 μM; 1 hour), followed by the addition of ET1 (0.1 μM; 4 hours) in media containing palmitate/BSA (200 μM) as substrate. Results are presented as representative fluorescent images and percent of normalized red/green fluorescence ratio versus control (open bar). A, The ability of ET1 to induce mitochondrial membrane depolarization, indicated by decreased ratio of JC-1 aggregated red signal to monomeric green signal, was attenuated by pretreatment with CB-13. B, Rescue of mitochondrial membrane potential by CB-13 was unaffected by compound C (data not shown). n = 7–8 (≥3 replicates per n-value). *$P < 0.05$ and **$P < 0.01$ versus control (open bars); †$P < 0.05$ versus ET1. Mean ± SEM.

$P < 0.01$ vs. control). We next performed knockdown of AMPK$\alpha_{1/2}$ to ascertain its contribution to CB-13 effects. Infection of cardiomyocytes with lentiviral constructs expressing shRNA against AMPKα_1 and AMPKα_2 produced significant and simultaneous reductions in AMPKα_1 and AMPKα_2 (see **Figure S5**, **Supplemental Digital Content 1**, http://links.lww.com/JCVP/A425). shRNA knockdown of AMPKα_1 and AMPKα_2 abrogated the ability of CB-13 to increase PGC-1α (Fig. 4B); in fact, CB-13 then reduced PGC-1α expression, whether in the presence (32% ± 7%; $P < 0.01$ vs. control) or absence (59% ± 10%; $P < 0.01$ vs. control) of ET1 (Fig. 4B).

We next examined CPT-1, which is a rate-limiting enzyme that facilitates the transport of fatty acids into the mitochondria for use as energy substrates.[41] CPT-1β, the predominant isoform of CPT-1 in the heart,[42] was assessed by real-time PCR. ET1 reduced CPT-1β expression to 82% ± 4% ($P < 0.05$ vs. control), and this was attenuated by CB-13 (91% ± 6%, ns from control or ET1) (Fig. 4C). However, simultaneous knockdown of AMPKα_1 and AMPKα_2 abrogated the ability of CB-13 to rescue CPT-1β (73% ± 8%; $P < 0.05$ vs. control) (Fig. 4C).

DISCUSSION

Mitochondrial aberrations have been linked to numerous aspects of cardiovascular disease, such as ischemia reperfusion injury,[21] cardiomyopathy,[22] and heart failure.[24] In fact, mitochondrial dysfunction purportedly contributes to the development of cardiac hypertrophy vis-à-vis, for example, altered mitochondrial biogenesis, decreased energy production/state, worsened redox status, and impaired Ca^{2+} homeostasis. Accordingly, improvement in mitochondrial function has been proposed as a therapeutic target toward the treatment of cardiac hypertrophy.[43] The present study shows that the activation of the endocannabinoid system

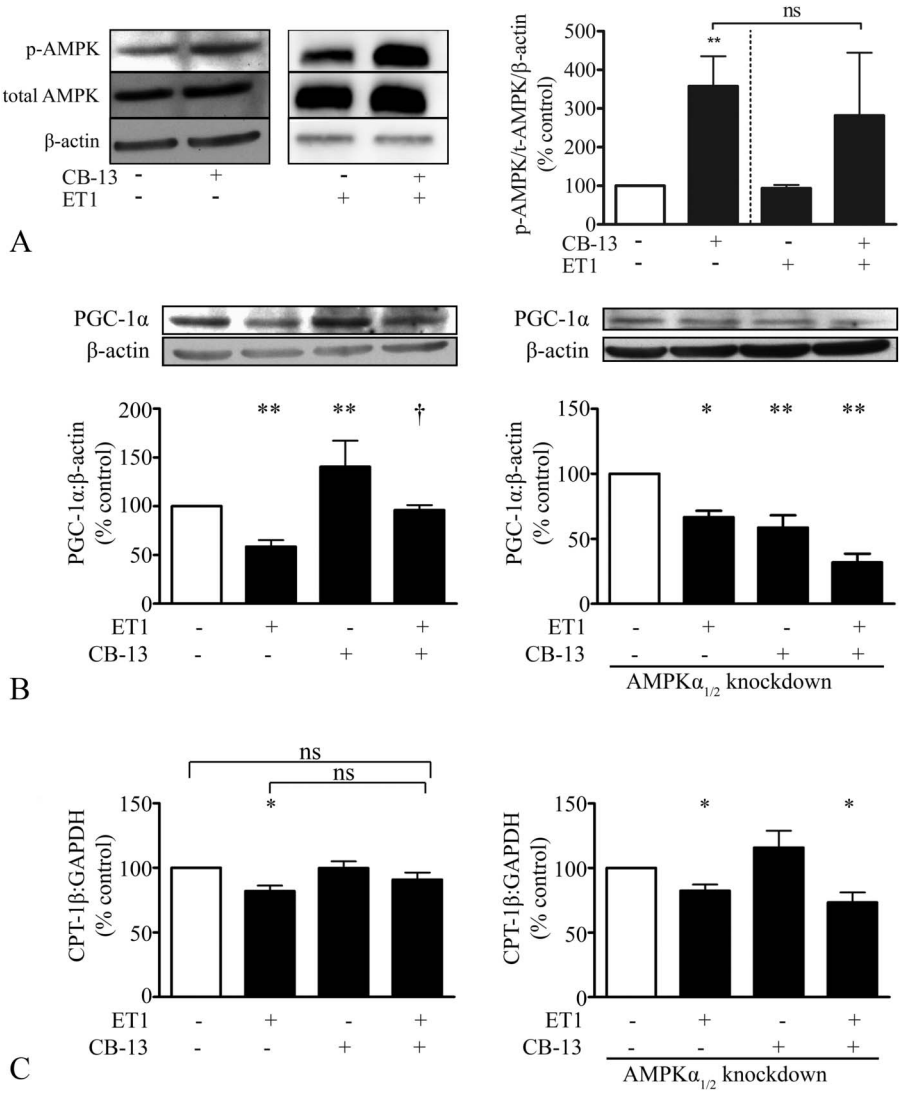

FIGURE 4. ET1-induced downregulation of PGC-1α, and CPT-1β is attenuated by CB-13 in an AMPK-dependent manner. A, Exposure to CB-13 (1 μM) significantly increased phosphorylation of AMPKα at Thr172, which is an indicator of AMPK activation status. AMPK phosphorylation in the presence of CB-13, and ET1 is comparable to AMPK phosphorylation levels in the presence of CB-13 alone. n = 3–9. $^{**}P < 0.01$ versus control (open bar). B, PGC-1α was reduced by ET1 (0.1 μM; 4 hours), and this was prevented by CB-13. Upregulation of PGC-1α by CB-13 in untreated myocytes was abolished by AMPKα_1/α_2 knockdown. Likewise, the ability of CB-13 to restore PGC-1α expression in ET1-treated myocytes was blocked by AMPKα_1/α_2 knockdown. n = 3–12. $^{*}P < 0.05$ and $^{**}P < 0.01$ versus control (open bars); †$P < 0.05$ versus ET1. C, ET1 decreased CPT-1β RNA expression, and this was partially attenuated by CB-13. AMPKα_1/α_2 knockdown blocked CB-13 effects. n = 5–8 (≥3 replicates per n value). $^{*}P < 0.05$ versus control (open bars); ns = not significant versus control (open bars). Mean ± SEM.

attenuates mitochondrial aberrations in cardiac myocytes subjected to an acute, prehypertrophic exposure of ET1. CB-13, a dual CB1/CB2 receptor agonist,[30,31] attenuated ET1-induced depression of fatty acid–dependent respiration (a surrogate marker of FAO), mitochondrial mPT, and mitochondrial inner membrane depolarization These protective effects of CB-13 were largely dependent on AMPK and were associated with rescued expression of 2 key regulators of mitochondrial function: PGC-1α and CPT-1β.

Acute Exposure to ET1 Impairs FAO-dependent Mitochondrial Bioenergetics

Our data suggest that an early response to ET1 is depressed FAO. ET1 reduced palmitate-dependent basal OCR (Fig. 1). This was attributable solely to a decrease in ATP-linked OCR and translated into compromised coupling efficiency (ie, efficiency of ATP production).

In ET1-treated cardiac myocytes, the net result of depressed FAO is a decrease in oxidative phosphorylation, yet hypertrophic growth, for example, is an energy-consuming process. From a bioenergetic perspective, this may explain, at least in part, the contribution of prolonged hypertrophy to the development of heart failure and functional decompensation.[44–46] We previously reported that ET1 impaired contractile function of cardiac myocytes by reducing shortening and relengthening velocities,[16] and a link exists between decreased conduction velocities, mitochondrial dysfunction, and inefficient cellular ATP utilization.[47,48] Moreover, maximal and spare respiration capacities, which reflect the ability of mitochondria to respond to higher energy demand, were also reduced by ET1. This predicts a limited capacity to adjust to conditions such as hemodynamic overload that require extra ATP, rendering myocytes vulnerable to secondary stress.[32]

Mitochondrial Membrane Integrity in ET1-Treated Cardiac Myocytes in the Presence of Palmitate

Mitochondrial $\Delta\psi_m$ results from the electrochemical gradient across the inner membrane, which is established as protons are pumped from the mitochondrial matrix to the intermembrane space by ETC complexes I, III, and IV (extrusion). In contrast, $\Delta\psi_m$ might be dissipated via proton leak and the ATP synthase pore (reentry). Thus, $\Delta\psi_m$ is influenced by the rates of proton extrusion and reentry.

Our data suggest that ET1-induced mitochondrial depolarization was attributable to reductions in proton extrusion (Fig. 3). In the presence of palmitate, ET1 reduced net proton reentry (as evidenced by reduced ATP-linked OCR and unaffected proton leak; Fig. 1). Nevertheless, mitochondrial $\Delta\psi_m$ was reduced, indicating that the decline in proton extrusion exceeded the decline in proton reentry. Thus, dissipation of $\Delta\psi_m$ was because of the reduction in active proton extrusion.

CB-13 restored $\Delta\psi_m$ in ET1-treated myocytes, and this appeared to be AMPK independent (Fig. 3). In the latter, the failure of compound C to abolish protective CB-13 effects on $\Delta\psi_m$ does not seem to reconcile with ablation of CB-13 effects on ATP-linked OCR (ie, proton reentry; Fig. 1C). This disparity might be explained by a concomitant further decrease in proton extrusion, where treatment with ET1 + compound C + CB-13 reduced not only proton re-entry via ATP synthase (Fig. 1C) but also proton extrusion. This would yield a normalized mitochondrial $\Delta\psi_m$. This might be achieved by a blunting of ETC complexes I, III, and IV expression and/or activity in the absence of AMPK signaling. Decreased AMPK activity and ETC complex expression were observed in pulmonary artery endothelial cells from fetal lambs with persistent pulmonary hypertension.[49] Decreased AMPK activity[50,51] and reduced gene expression of complex I and ATP synthase were also detected in rat ventricles,[52] and in the spontaneously hypertensive rat, hypertrophy is linked to suppressed activities of complex I and AMPK.[53] Another mechanism by which loss of AMPK might impair proton extrusion is via reduced CPT-1β levels, as shown in response to ET1 + CB-13 + AMPK knockdown treatment (Fig. 4C). Suppression of CPT-1β would reduce mitochondrial fatty acid uptake and entry into the tricarboxylic acid cycle, electron donor concentrations ($NADH/FADH_2$), and therefore ETC-dependent proton extrusion. Thus, our findings suggest that during FAO, disrupting AMPK abolishes the ability of CB-13 to maintain both proton extrusion rate and proton reentry, yielding a net noneffect on mitochondrial $\Delta\psi_m$. Thus, rather than suggesting noninvolvement of AMPK, the inability of compound C to reverse CB-13 rescue of $\Delta\psi_m$ reflects a parallel loss of CB-13/AMPK effects on proton extrusion and reentry.

Effects of liganded CB receptor activation on mitochondrial signaling cascades is explained in **Supplemental Digital Content 1** (schematic representation, see **Figure S7**, http://links.lww.com/JCVP/A425).

We identified PGC-1α as a candidate mediator of CB-13 actions. PGC-1α is a key transcriptional coactivator that regulates mitochondrial function. ET1, angiotensin II, and phenylephrine in myocytes[54] or pressure overload in vivo[55] downregulate PGC-1α. Activators of AMPK increase PGC-1α expression, and when PGC-1α is absent, the expression of several target mitochondrial genes of AMPK is ablated.[56] AMPK might also stimulate PGC-1α by increasing NAD^+:-NADH, thereby activating sirtuin-1 (SIRT1), an NAD^+-dependent deacetylase. SIRT-1 activates PGC-1α by deacetylating lysine sites,[57,58] and AMPK and SIRT1 reciprocally upregulate each other.[59,60] PGC-1α regulates mitochondrial biogenesis, ATP synthesis, and ROS defense mechanisms,[61,62] and PGC-1α overexpression rescues cardiac mitochondrial function.[43] ET1 reduced PGC-1α and, consistent with reports that deactivation of the PPARγ/PGC-1α complex leads to downregulation of FAO genes,[57,63,64] CPT-1β expression (Fig. 4) as well. Upregulation of CPT-1 involves AMPK,[65] so while CB-13 rescued PGC-1α and CPT-1β expression, $AMPK\alpha_{1/2}$ knockdown abrogated CB-13 effects.

When we disrupted AMPK signaling, by shRNA knockdown or using compound C, CB-13 treatment alone reduced PGC-1α (Fig. 4B) and, as would then be expected, FAO-related mitochondrial respiration (Fig. 1). We speculate that CB-13 activates AMPK via CB2 receptors, whereas CB1 receptors invoke other signaling. JWH-133, a CB2-selective

agonist, activates AMPK (data not shown), and a CB2 agonist is sufficient to stimulate PGC-1α.[66] This suggests that without AMPK signaling, CB-13 might be stimulating other signaling cascades to reduce PGC-1α, thus depressing FAO-related mitochondrial bioenergetics. CB-13 is a dual agonist of CB1 and CB2 receptors; our previous findings showed that anandamide, which is equally potent at CB1 and CB2 receptors,[67] stimulates PGC-1α expression in the Sprague Dawley rat heart, and moreover, JWH-133 stimulates AMPK activity (data not shown). In addition, Zheng et al[66] reported that a CB2 agonist activated PGC-1α. Therefore, we speculate that CB1-induced signaling emerges to exert opposing effects when CB2/AMPK signaling is inhibited. Indeed, Tedesco et al[68] observed decreased AMPK activity and endothelial nitric oxide synthase expression, as well as depressed mitochondrial biogenesis in liver, muscle, and white adipose tissues in mice treated with a CB1-selective agonist. Perwitz et al[69] also showed that blockage of CB1 receptors enhanced mitochondrial respiration and increased AMPK activity and PGC-1α expression in adipocytes. Other studies also reported the opposite effects of CB1 and CB2 receptors, where CB1 is detrimental and CB2 is beneficial.[70–72] Therefore, an explanation for our finding that CB-13 impairs FAO when AMPK signaling is inhibited might be that CB1 (deleterious) and CB2 (salutary) act in opposition, at least in cardiac myocyte mitochondria, and that CB2 receptor–stimulated AMPK pathways dominate over CB1 receptor signaling in cardiac myocytes to achieve regulation of mitochondrial function by CB-13. This remains to be tested.

CONCLUSIONS

We previously reported that manipulation of the endocannabinoid system represents a viable strategy to prevent cardiac hypertrophy.[16] Here, activation of CB receptors exerted early protective effects on mitochondrial function in cardiac myocytes exposed to a prohypertrophic agonist. Dual agonism of CB1 and CB2 receptors restored mitochondrial $\Delta\psi_m$ and prevented depression of FAO-related mitochondrial bioenergetics. AMPK played a central role, at least in part by upregulating PGC-1α and CPT-1β, which are key regulators of FAO. Given that fatty acids are the primary energy source in the heart, the ability of CB-13 to restore FAO strengthens its cardioprotective potential. Thus, activation of peripheral CB1/CB2 receptors may be a new therapeutic approach to address mitochondrial dysfunction in the context of cardiac disease.

ACKNOWLEDGMENTS

The authors are grateful to Dr Zongjun Shao for her excellent technical assistance.

REFERENCES

1. Bonz A, Laser M, Kullmer S, et al. Cannabinoids acting on CB1 receptors decrease contractile performance in human atrial muscle. *J Cardiovasc Pharmacol.* 2003;41:657–664.
2. Bouchard JF, Lepicier P, Lamontagne D. Contribution of endocannabinoids in the endothelial protection afforded by ischemic preconditioning in the isolated rat heart. *Life Sci.* 2003;72:1859–1870.
3. Gebremedhin D, Lange AR, Campbell WB, et al. Cannabinoid CB1 receptor of cat cerebral arterial muscle functions to inhibit L-type Ca2+ channel current. *Am J Physiol.* 1999;276:H2085–H2093.
4. Liu J, Gao B, Mirshahi F, et al. Functional CB1 cannabinoid receptors in human vascular endothelial cells. *Biochem J.* 2000;346 Pt 3:835–840.
5. Matsuda LA, Lolait SJ, Brownstein MJ, et al. Structure of a cannabinoid receptor and functional expression of the cloned cDNA. *Nature.* 1990; 346:561–564.
6. Munro S, Thomas KL, Abu-Shaar M. Molecular characterization of a peripheral receptor for cannabinoids. *Nature.* 1993;365:61–65.
7. Devane WA, Hanus L, Breuer A, et al. Isolation and structure of a brain constituent that binds to the cannabinoid receptor. *Science.* 1992;258: 1946–1949.
8. Mechoulam R, Ben-Shabat S, Hanus L, et al. Identification of an endogenous 2-monoglyceride, present in canine gut, that binds to cannabinoid receptors. *Biochem Pharmacol.* 1995;50:83–90.
9. Deutsch DG, Chin SA. Enzymatic synthesis and degradation of anandamide, a cannabinoid receptor agonist. *Biochem Pharmacol.* 1993;46: 791–796.
10. Maccarrone M, van der Stelt M, Rossi A, et al. Anandamide hydrolysis by human cells in culture and brain. *J Biol Chem.* 1998;273:32332–32339.
11. Deutsch DG, Goligorsky MS, Schmid PC, et al. Production and physiological actions of anandamide in the vasculature of the rat kidney. *J Clin Invest.* 1997;100:1538–1546.
12. Pacher P, Batkai S, Kunos G. The endocannabinoid system as an emerging target of pharmacotherapy. *Pharmacol Rev.* 2006;58:389–462.
13. Underdown NJ, Hiley CR, Ford WR. Anandamide reduces infarct size in rat isolated hearts subjected to ischaemia-reperfusion by a novel cannabinoid mechanism. *Br J Pharmacol.* 2005;146:809–816.
14. Lepicier P, Bouchard JF, Lagneux C, et al. Endocannabinoids protect the rat isolated heart against ischaemia. *Br J Pharmacol.* 2003;139:805–815.
15. Lagneux C, Lamontagne D. Involvement of cannabinoids in the cardioprotection induced by lipopolysaccharide. *Br J Pharmacol.* 2001;132: 793–796.
16. Lu Y, Akinwumi BC, Shao Z, et al. Ligand activation of cannabinoid receptors attenuates hypertrophy of neonatal rat cardiomyocytes. *J Cardiovasc Pharmacol.* 2014;64:420–430.
17. Lopaschuk GD, Ussher JR, Folmes CD, et al. Myocardial fatty acid metabolism in health and disease. *Physiol Rev.* 2010;90:207–258.
18. Opie LH. Metabolism of the heart in health and disease. I. *Am Heart J.* 1968;76:685–698.
19. Ashrafian H, Frenneaux MP, Opie LH. Metabolic mechanisms in heart failure. *Circulation.* 2007;116:434–448.
20. Kolwicz SC Jr, Purohit S, Tian R. Cardiac metabolism and its interactions with contraction, growth, and survival of cardiomyocytes. *Circ Res.* 2013;113:603–616.
21. Stanley WC. Myocardial energy metabolism during ischemia and the mechanisms of metabolic therapies. *J Cardiovasc Pharmacol Ther.* 2004;9(suppl 1):S31–S45.
22. Taylor D, Bhandari S, Seymour AM. Mitochondrial dysfunction in uremic cardiomyopathy. *Am J Physiol Renal Physiol.* 2015;308:F579–F587.
23. Doenst T, Pytel G, Schrepper A, et al. Decreased rates of substrate oxidation ex vivo predict the onset of heart failure and contractile dysfunction in rats with pressure overload. *Cardiovasc Res.* 2010;86:461–470.
24. Doenst T, Nguyen TD, Abel ED. Cardiac metabolism in heart failure: implications beyond ATP production. *Circ Res.* 2013;113:709–724.
25. Wu J, LaPointe MC, West BL, et al. Tissue-specific determinants of human atrial natriuretic factor gene expression in cardiac tissue. *J Biol Chem.* 1989;264:6472–6479.
26. Alibin CP, Kopilas MA, Anderson HD. Suppression of cardiac myocyte hypertrophy by conjugated linoleic acid: role of peroxisome proliferator-activated receptors alpha and gamma. *J Biol Chem.* 2008;283:10707–10715.
27. Zhang H, Shao Z, Alibin CP, et al. Liganded peroxisome proliferator-activated receptors (PPARs) preserve nuclear histone deacetylase 5 levels in endothelin-treated sprague-dawley rat cardiac myocytes. *PLoS One.* 2014;9:e115258.
28. Huang Y, Zhang H, Shao Z, et al. Suppression of endothelin-1-induced cardiac myocyte hypertrophy by PPAR agonists: role of diacylglycerol kinase zeta. *Cardiovasc Res.* 2011;90:267–275.

29. Sun X, Kumar S, Sharma S, et al. Endothelin-1 induces a glycolytic switch in pulmonary arterial endothelial cells via the mitochondrial translocation of endothelial nitric oxide synthase. *Am J Respir Cell Mol Biol.* 2014;50:1084–1095.
30. Dziadulewicz EK, Bevan SJ, Brain CT, et al. Naphthalen-1-yl-(4-pentyloxynaphthalen-1-yl)methanone: a potent, orally bioavailable human CB1/CB2 dual agonist with antihyperalgesic properties and restricted central nervous system penetration. *J Med Chem.* 2007;50:3851–3856.
31. Cluny NL, Keenan CM, Duncan M, et al. Naphthalen-1-yl-(4-pentyloxynaphthalen-1-yl)methanone (SAB378), a peripherally restricted cannabinoid CB1/CB2 receptor agonist, inhibits gastrointestinal motility but has no effect on experimental colitis in mice. *J Pharmacol Exp Ther.* 2010;334:973–980.
32. Roy Chowdhury SK, Smith DR, Saleh A, et al. Impaired adenosine monophosphate-activated protein kinase signalling in dorsal root ganglia neurons is linked to mitochondrial dysfunction and peripheral neuropathy in diabetes. *Brain J Neurol.* 2012;135:1751–1766.
33. Brand MD, Nicholls DG. Assessing mitochondrial dysfunction in cells. *Biochem J.* 2011;435:297–312.
34. Hill BG, Dranka BP, Zou L, et al. Importance of the bioenergetic reserve capacity in response to cardiomyocyte stress induced by 4-hydroxynonenal. *Biochem J.* 2009;424:99–107.
35. Petronilli V, Miotto G, Canton M, et al. Transient and long-lasting openings of the mitochondrial permeability transition pore can be monitored directly in intact cells by changes in mitochondrial calcein fluorescence. *Biophysical J.* 1999;76:725–734.
36. Luiken JJ, Coort SL, Willems J, et al. Contraction-induced fatty acid translocase/CD36 translocation in rat cardiac myocytes is mediated through AMP-activated protein kinase signaling. *Diabetes.* 2003;52:1627–1634.
37. Makinde AO, Gamble J, Lopaschuk GD. Upregulation of 5'-AMP-activated protein kinase is responsible for the increase in myocardial fatty acid oxidation rates following birth in the newborn rabbit. *Circ Res.* 1997;80:482–489.
38. Witters LA, Kemp BE, Means AR. Chutes and Ladders: the search for protein kinases that act on AMPK. *Trends Biochem Sci.* 2006;31:13–16.
39. Beauloye C, Bertrand L, Horman S, et al. AMPK activation, a preventive therapeutic target in the transition from cardiac injury to heart failure. *Cardiovasc Res.* 2011;90:224–233.
40. Wu Z, Boss O. Targeting PGC-1 alpha to control energy homeostasis. *Expert Opin Ther Targets.* 2007;11:1329–1338.
41. Kerner J, Hoppel C. Fatty acid import into mitochondria. *Biochim Biophys Acta.* 2000;1486:1–17.
42. Brown NF, Weis BC, Husti JE, et al. Mitochondrial carnitine palmitoyltransferase I isoform switching in the developing rat heart. *J Biol Chem.* 1995;270:8952–8957.
43. Zhou LY, Liu JP, Wang K, et al. Mitochondrial function in cardiac hypertrophy. *Int J Cardiol.* 2013;167:1118–1125.
44. Levy D, Garrison RJ, Savage DD, et al. Prognostic implications of echocardiographically determined left ventricular mass in the Framingham Heart Study. *New Engl J Med.* 1990;322:1561–1566.
45. Ho KK, Pinsky JL, Kannel WB, et al. The epidemiology of heart failure: the Framingham Study. *J Am Coll Cardiol.* 1993;22(4 suppl A):6A–13A.
46. Berenji K, Drazner MH, Rothermel BA, et al. Does load-induced ventricular hypertrophy progress to systolic heart failure? *Am J Physiol.* 2005;289:H8–H16.
47. Zhang Y, Yuan M, Bradley KM, et al. Insulin-like growth factor 1 alleviates high-fat diet-induced myocardial contractile dysfunction: role of insulin signaling and mitochondrial function. *Hypertension.* 2012;59:680–693.
48. Luedde M, Flogel U, Knorr M, et al. Decreased contractility due to energy deprivation in a transgenic rat model of hypertrophic cardiomyopathy. *J Mol Med.* 2009;87:411–422.
49. Afolayan AJ, Eis A, Alexander M, et al. Decreased endothelial NOS expression and function contributes to impaired mitochondrial biogenesis and oxidative stress in fetal lambs with PPHN. *Am J Physiol Lung Cell Mol Physiol.* 2015;310:L40–L49.
50. Zhang Y, Mi SL, Hu N, et al. Mitochondrial aldehyde dehydrogenase 2 accentuates aging-induced cardiac remodeling and contractile dysfunction: role of AMPK, Sirt1, and mitochondrial function. *Free Radic Biol Med.* 2014;71:208–220.
51. Salminen A, Kaarniranta K. AMP-activated protein kinase (AMPK) controls the aging process via an integrated signaling network. *Ageing Res Rev.* 2012;11:230–241.
52. Preston CC, Oberlin AS, Holmuhamedov EL, et al. Aging-induced alterations in gene transcripts and functional activity of mitochondrial oxidative phosphorylation complexes in the heart. *Mech Ageing Dev.* 2008;129:304–312.
53. Tang Y, Mi C, Liu J, et al. Compromised mitochondrial remodeling in compensatory hypertrophied myocardium of spontaneously hypertensive rat. *Cardiovasc Pathol official J Soc Cardiovasc Pathol.* 2014;23:101–106.
54. Garnier A, Zoll J, Fortin D, et al. Control by circulating factors of mitochondrial function and transcription cascade in heart failure: a role for endothelin-1 and angiotensin II, Circulation. *Heart Fail.* 2009;2:342–350.
55. Garnier A, Fortin D, Delomenie C, et al. Depressed mitochondrial transcription factors and oxidative capacity in rat failing cardiac and skeletal muscles. *J Physiol.* 2003;551:491–501.
56. Jager S, Handschin C, St-Pierre J, et al. AMP-activated protein kinase (AMPK) action in skeletal muscle via direct phosphorylation of PGC-1alpha. *Proc Natl Acad Sci U S A.* 2007;104:12017–12022.
57. Rodgers JT, Lerin C, Haas W, et al. Nutrient control of glucose homeostasis through a complex of PGC-1alpha and SIRT1. *Nature.* 2005;434:113–118.
58. Lu P, Kamboj A, Gibson SB, et al. Poly(ADP-ribose) polymerase-1 causes mitochondrial damage and neuron death mediated by Bnip3. *J Neurosci.* 2014;34:15975–15987.
59. Lan F, Cacicedo JM, Ruderman N, et al. SIRT1 modulation of the acetylation status, cytosolic localization, and activity of LKB1. Possible role in AMP-activated protein kinase activation. *J Biol Chem.* 2008;283:27628–27635.
60. Jiang S, Wang W, Miner J, et al. Cross regulation of sirtuin 1, AMPK, and PPARgamma in conjugated linoleic acid treated adipocytes. *PLoS One.* 2012;7:e48874.
61. Ventura-Clapier R, Garnier A, Veksler V. Transcriptional control of mitochondrial biogenesis: the central role of PGC-1alpha. *Cardiovasc Res.* 2008;79:208–217.
62. St-Pierre J, Drori S, Uldry M, et al. Suppression of reactive oxygen species and neurodegeneration by the PGC-1 transcriptional coactivators. *Cell.* 2006;127:397–408.
63. Lehman JJ, Kelly DP. Transcriptional activation of energy metabolic switches in the developing and hypertrophied heart. *Clin Exp Pharmacol Physiol.* 2002;29:339–345.
64. Planavila A, Iglesias R, Giralt M, et al. Sirt1 acts in association with PPARalpha to protect the heart from hypertrophy, metabolic dysregulation, and inflammation. *Cardiovasc Res.* 2011;90:276–284.
65. Li L, Wu L, Wang C, et al. Adiponectin modulates carnitine palmitoyltransferase-1 through AMPK signaling cascade in rat cardiomyocytes. *Regul Pept.* 2007;139:72–79.
66. Zheng X, Sun T, Wang X. Activation of type 2 cannabinoid receptors (CB2R) promotes fatty acid oxidation through the SIRT1/PGC-1alpha pathway. *Biochem biophysical Res Commun.* 2013;436:377–381.
67. Felder CC, Joyce KE, Briley EM, et al. Comparison of the pharmacology and signal transduction of the human cannabinoid CB1 and CB2 receptors. *Mol Pharmacol.* 1995;48:443–450.
68. Tedesco L, Valerio A, Dossena M, et al. Cannabinoid receptor stimulation impairs mitochondrial biogenesis in mouse white adipose tissue, muscle, and liver: the role of eNOS, p38 MAPK, and AMPK pathways. *Diabetes.* 2010;59:2826–2836.
69. Perwitz N, Wenzel J, Wagner I, et al. Cannabinoid type 1 receptor blockade induces transdifferentiation towards a brown fat phenotype in white adipocytes. *Diabetes Obes Metab.* 2010;12:158–166.
70. Li Q, Guo HC, Maslov LN, et al. Mitochondrial permeability transition pore plays a role in the cardioprotection of CB2 receptor against ischemia-reperfusion injury. *Can J Physiol Pharmacol.* 2014;92:205–214.
71. Li Q, Wang F, Zhang YM, et al. Activation of cannabinoid type 2 receptor by JWH133 protects heart against ischemia/reperfusion-induced apoptosis. *Cell Physiol Biochem Int J Exp Cell Physiol Biochem Pharmacol.* 2013;31:693–702.
72. Fisar Z, Singh N, Hroudova J. Cannabinoid-induced changes in respiration of brain mitochondria. *Toxicol Lett.* 2014;231:62–71.